JOURNAL OF APPLIED ELECTROCHEMISTRY 22 (1992) 247–254

Corrosion behaviour of electrogalvanized steel in sodium chloride and ammonium sulphate solutions; a study by E.I.S.

L. FEDRIZZI, L. CIAGHI, P. L. BONORA

Dipartimento di Ingegneria dei Materiali, Università di Trento, 38050 Mesiano di Povo, Trento, Italy

R. FRATESI*, G. ROVENTI

Dipartimento di Scienze dei Materiali e della Terra, Università di Ancona, Via Brecce Bianche, 60131 Ancona, Italy

Received 21 January 1991; revised 26 June 1991

Zinc and zinc–nickel (13% Ni) electrodeposits were passivated by dipping in chromate baths and characterized by scanning electron microscopy. The corrosion behaviour was studied using a.c. electrochemical techniques; electrochemical impedance spectroscopy (EIS) measurements were performed at open circuit and under galvanostatic control during the 24 h immersion time. In sodium chloride solution the zinc–nickel electrodeposits show a better corrosion resistance compared to the pure zinc coatings. During the immersion time, a surface nickel enrichment was observed which, together with the zinc corrosion products, acts as a barrier layer reducing the total corrosion rate. In the same solution the passivation treatment improves the corrosion resistance of the electrodeposits; nevertheless, on zinc substrates, the protection exerted by the chromate film is not always effective during the immersion time. On the contrary the chromate coating on zinc–nickel substrates induces a remarkable and durable improvement of the corrosion resistance, reducing the zinc dissolution almost completely. In the ammonium sulphate solution, the corrosion mechanism is significantly influenced by hydrogen reduction on the zinc–nickel surfaces, and by the production of a local surface acidity which is aggressive for the chromate coatings.

1. Introduction

Numerous changes have been taking place in the production of zinc coatings on steel to improve the corrosion resistance using zinc alloy plating. For this purpose, attention was focused on processes aimed at obtaining multilayer galvanic coatings [1, 2], composite zinc films [3, 4] and electrodeposited coatings of zinc alloys using the 8th group metals [5–11]. Among the latter, zinc–nickel alloys (8–14% Ni) are the most successful; in fact they show better corrosion resistance compared to the zinc coatings in laboratory accelerated tests [8–12].

There is a considerable record of data on zinc corrosion obtained by electrochemical tests in acid, alkaline or neutral media [13–15]. By contrast only data from salt spray tests are available for the corrosion resistance of electrodeposited zinc alloys.

In a previous work [16], the corrosion resistance of zinc and zinc–nickel alloy (13% Ni), with or without chromate treatment, was studied. This study was carried out by means of a Tafel line extrapolation procedure and a polarization resistance technique in 0.6 M NaCl and 0.1 M $(NH_4)_2SO_4$ solutions, both in aerated and deaerated conditions. Because impedance measurements carried out over a wide frequency range are particularly relevant in the investigation of electrode reactions, these were used in the present work.

In particular, the Tafel line extrapolation technique causes irreversible surface changes, and polarization d.c. measurements have certain problems such as uncompensated ohmic resistance and adsorption of species on the electrode surface [17]. However, impedence measurements avoid irreversible changes in the system, allowing a determination of the ohmic resistance and yielding the double layer capacitance.

In this work, data obtained by the a.c. impedance technique are also compared with the results obtained in previous work [16] where the d.c. polarization technique was used.

2. Experimental details

Zinc and zinc–nickel (13% Ni) electrodeposits, about 10 μm thick, were obtained on both sides of mild steel discs, 1 mm thick, from chloride baths in galvanostatic conditions. The exposed area was approximately 15 cm^2. The geometry of the electrolytic cell as well as

* To whom all correspondence should be addressed.

0021-891X/92

the composition of the baths and electrodeposition conditions have been reported previously [12–18]. The electrodeposited zinc samples were passivated by dipping, for 10 s at 25° C, in a solution containing 2 g dm^{-3} Cr^{6+} and 10 g dm^{-3} HNO_3. The zinc–nickel samples were passivated by dipping, for 2 min at 35° C, in a solution containing 25 g dm^{-3} Cr^{6+} at pH = 1.8 (HCl). After dipping, the samples were washed and dried using hot air (max 60° C), and left for 24 h prior to the electrochemical measurements.

The microstructural characterization was performed using a scanning electron microscope (SEM) and surface microanalysis was performed by energy dispersive X-ray spectroscopy (EDXS).

At immersion, a sample E_{corr} was measured and recorded against time until its change over a one hour period was less than 10 mV.

The corrosion behaviour was studied by a.c. electrochemical techniques. Electrochemical impedance spectroscopy (EIS) measurements were performed at open circuit and under galvanostatic control during the immersion time of 24 h. The a.c. current signal was the smallest possible in order to obtain a corrosion potential (E_{corr}) change lower than 5 mV. The impedance measurements, in the range 10 kHz–10 mHz, were carried out using a Solartron 1250 frequency response analyzer coupled with a Solartron 1286 electrochemical interface.

The test environments employed were a 3.5% NaCl (pH 6.4) and a 0.1 M $(NH_4)_2SO_4$ (pH 5.9) solutions in aerated and dearated conditions. When tests were performed in deaerated media, the solution, prior to the sample immersion, was deaerated for at least 1 h by argon bubbling; during the measurements the flux of argon was maintained above the solution level.

The cell used was a conventional ASTM glass vessel. A flat specimen holder, as suggested by the ASTM standard, leaving an exposed area of 4 cm^2, was used. The reference electrode was a saturated calomel electrode (SCE) for chloride solution and a saturated sulphate electrode (SSE) for the ammonium sulphate solution. A platinum counterelectrode was used and maintained separate from the working solution by fritted glass. All measurements were performed in quiescent electrolytes at 25 ± 1° C.

3. Results and discussion

The coatings appear homogeneous and fine grained; moreover, no defects or inclusions are present. The zinc–nickel electrodeposits show a columnar and pyramidal structure of crystal grains (Fig. 1) which appear more rounded after the chromate treatment. Moreover, after chromate treatment, some narrow and deep cracks are visible (Fig. 2). These cracks were well characterized previously [19] and quite similar to those observed by Lambert [20] after the corrosive attack of a zinc–nickel coating in NaCl solutions. The chromate bath (pH 1.8) and the long treatment time (2 min) may induce the small corrosion phenomena observed.

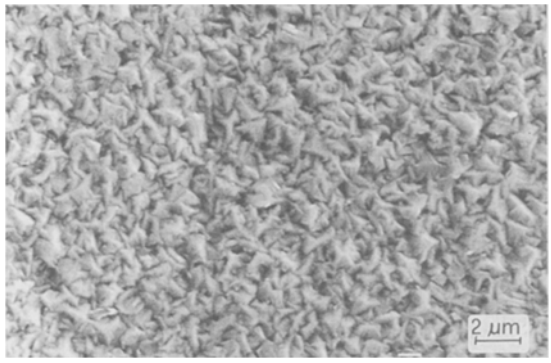

Fig. 1. Microstructure of the zinc–nickel electrodeposited alloy.

The electrochemical measurements were carried out as soon as the corrosion potential (E_{corr}) was stable. The E_{corr} values are shown in Table 1. The E_{corr} of the zinc–nickel alloy is more noble with respect to the zinc electrodeposit in all the solutions used. Moreover, this potential becomes nobler the longer the immersion time, as a consequence of a surface nickel enrichment [20]. However, no evident effect on the corrosion potential derives from the passivation treatment.

Furthermore, the E_{corr} of all the samples becomes more active when the solution is deaerated as a consequence of the non depolarization of the oxygen cathodic reaction. This phenomenon is evident in the sodium chloride solution. However, the shift of E_{corr} is not so clear for the zinc–nickel alloy samples in the ammonium sulphate solution, where the cathodic current is supported by reactions involving the ammonium ions [13]. These reactions appear more active on the nickel containing surfaces.

3.1. *Aerated sodium chloride solution*

The Nyquist impedance diagrams obtained in the aerated 3.5% NaCl solution are shown in Fig. 3. In Table 2 the resistance (R) and the capacity (C) values, deriving from the impedance spectra analysis [21] were collected. The impedance plots relevant to the zinc electrocoatings (Fig. 3a) show a well defined capacitative loop. Due to the experimental conditions, no evidence of other inductive or capacitative loops at the lowest frequencies (up to 10 mHz) were found.

It is known that, if the process is purely charge

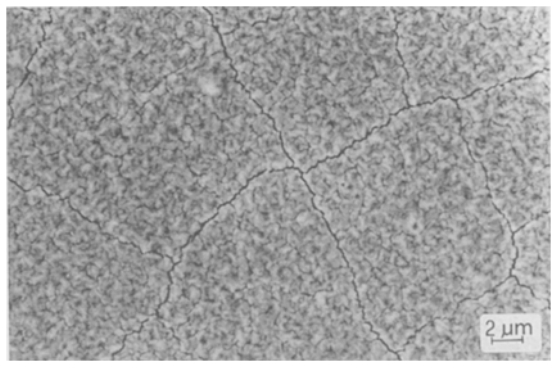

Fig. 2. Microstructure of the zinc–nickel electrodeposited alloy after the chromate treatment.

Table 1. Corrosion potentials (mV/SCE) of the various materials in the two considered solutions

Material	*Time (h)*	*NaCl*		*$(NH_4)_2SO_4$*	
		Aerated	*Deaerated*	*Aerated*	*Deaerated*
Zn	3	−1078	−1187	−1056	−1143
Zn–Ni	3	−881	−950	−977	−996
	24	−854	−930	−881	−857
Chromated Zn	3	−1055	−1182	−1061	−1148
Chromated Zn–Ni	3	−870	−940	−983	−957
	24	−816	−921	−863	−886

transfer controlled, the impedance spectrum will be a perfect semicircle [22]; the shape of the impedance plot relevant to the zinc electrodeposits, suggests that zinc corrosion occurs under charge transfer control as indicated by other authors [23, 24]. The shape of the impedance spectra supports the assumption that the polarization resistance (R_p) value is the same as the charge transfer resistance (R_{ct}), which is easily estimated on the real impedance axis by extrapolating the impedance trend at the lowest frequencies. In this way R_{ct} values of about $1100\,\Omega\,cm^2$ were recorded; these agree with the R_p data obtained by d.c. electrochemical methods in our previous work [16, 19, 25]. The electrochemical behaviour seems to be unchanged during the 24 h of immersion; nevertheless a small increase in the R_{ct} value is observed, the impedance data being shifted towards the low frequency portion. This trend may indicate some mass transfer problems related to the presence of corrosion products on the samples surface [26, 27]. The capacity value shows a remarkable increase during the immersion time (from 70 to $300\,\mu F\,cm^{-2}$). After 24 h of immersion, the measured capacity is not related to a double layer capacity (C_{dl}), confirming the presence of porous corrosion products, which, by X-ray diffraction, were found to be ZnO and $ZnCl_2 \cdot 4Zn(OH)_2$. Moreover, the capacity increase may also be correlated to an increase in the microscopic area due to the corrosive attack [28].

The electrochemical parameters relevant to the zinc–nickel alloy (Fig. 3b), stabilize after several hours of immersion, and the R_{ct} reaches a value of about $3000\,\Omega\,cm^2$. These data are also in good agreement with the R_p values obtained by d.c. electrochemical methods [16]. The impedance diagram consists of an almost semicircular capacitive loop and its shape remains unchanged during the 24 h of immersion. However, the R_{ct} value shows a slight increase up to $3900\,\Omega\,cm^2$ which may be related to a surface nickel enrichment and to the presence of a barrier of zinc corrosion products. The contemporary increase in the capacity value (not related to a double layer capacity) supports the assumption of the presence of corrosion products.

These results agree with the zinc preferential dissolution mechanism, as proposed by Lambert for this type of alloy [20]. During dezincification the electro-

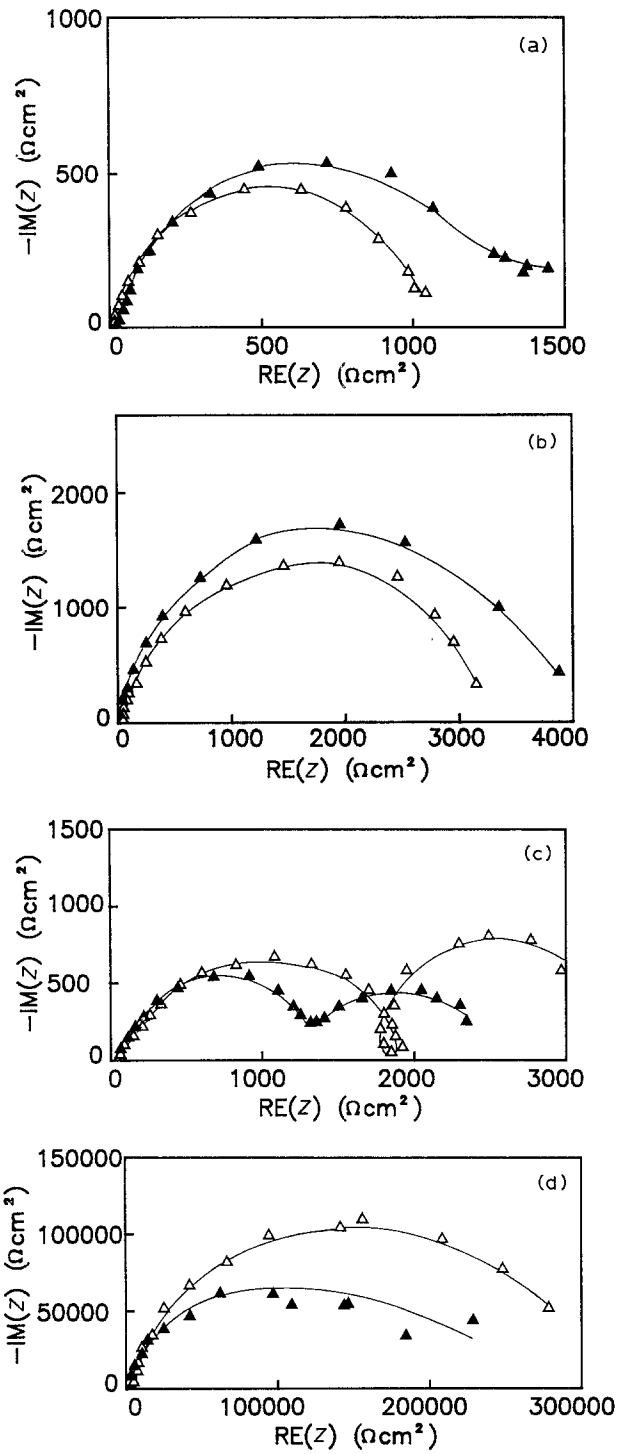

Fig. 3. Nyquist impedance plots obtained in aerated 3.5% NaCl solution after 3 (△) and 24 (▲) hours of immersion. (a) Zinc, (b) zinc–nickel, (c) chromated zinc and (d) chromated zinc–nickel.

deposit surface actually becomes a composite, composed of zinc corrosion products and of the underlying nickel enriched metallic phase. This coating offers a lower galvanic protection of the steel substrate and acts mainly as a barrier protection which corrodes more slowly compared to the zinc electrodeposit in the aerated NaCl solution, as indicated by the higher R_{ct} values.

The interpretation of the data relevant to the passivated materials is more difficult; the corrosion behaviour strictly depends on the production procedure [28]. The treatment time, the chromate bath

Table 2. Resistance, $R(\Omega cm^2)$, and capacity, $C(\mu F cm^{-2})$, values derived from the impedance spectra obtained in aerated and deaerated 3.5% NaCl solutions. Capacity values were calculated using the formula $C = 1/2\pi f_{max} R$

Material	*Time (h)*	*Aerated*		*Deaerated*	
		R	*C*	*R*	*C*
Zn	3	1100*	73	2700	39
	24	1400	291		
Zn–Ni	3	3100	81	5000	26
	24	3900	647		
Chromated Zn	3	1800*	5.6*	7500†	21
	3	1700	4246		
	24	1400*	72*		
	24	1000	26539		
Chromated Zn–Ni	3	320000	8	280000	5.7
	24	205000	7.7		

* Impedance diagram showing two capacitative loops.
† By extrapolating the first capacitative loop.

temperature and composition, the bath pH value are critical factors for the production of coatings with quality characteristics.

The impedance diagrams, relevant to passivated zinc electrodeposits (Fig. 3c), show two well defined capacitative loops. The real component of the impedance relevant to the first loop is in the region of $1800\,\Omega cm^2$ and the C value ranges around $6\,\mu F cm^{-2}$. This very low capacitance indicates that the first impedance loop is related to the presence of the chromium oxide coating [28]. The value of the real component of the impedance at the lowest frequencies (second loop) is about $3500\,\Omega cm^2$. This is in good agreement with the R_p data obtained by d.c. electrochemical methods [16]. The corrosion rate of the composite is therefore likely to be closely related to the trend of the lowest frequency value of the impedance plot.

In some samples, after the 24 h of immersion, a complete dissolution of the chromate deposit was observed and the impedance diagram became similar to that of the zinc electrocoating. In other cases, the two capacitative loops were still present; nevertheless, an increase in C_{dl} for the first loop up to $70\,\mu F cm^{-2}$ (similar to the typical value of the zinc coating) and the simultaneous decrease in total impedance was noted. This trend is also representative of the degradation of the protective properties of the chromate coating.

It can be deduced, therefore, that the passivation treatment improves the corrosion resistance of a zinc electrocoating, although in the aggressive NaCl solutions, the effectiveness of this treatment is not long-lasting. The behaviour of the passivated zinc–nickel electrocoatings is completely different (Fig. 3d). In fact, in this case the impedance diagram shows the presence of only one, very wide, capacitative loop, which remains almost unchanged during the 24 h of immersion. The R_{ct} values are in the range 10^5–$10^6\,\Omega cm^2$ and the C data are always lower than $10\,\mu F cm^{-2}$.

The capacity values indicate that the chromium oxide film is always present during the whole immersion time and that no corrosion products are growing on the surface. The very high R_{ct} data show that the chromate coating, acting as a barrier, exerts an effective corrosion protection in the NaCl solution, probably inhibiting the anodic dissolution on the whole surface and also on the zones where the coating shows some narrow cracks. Both the d.c. and a.c. electrochemical methods show very good corrosion resistance of the chromated zinc–nickel electrodeposits [16]. The amount of Cr retained on the sample surface, after the passivation treatment, is almost the same as that measured on the surface of the chromate treated zinc electrocoatings. However, the chromate treatment of zinc–nickel alloy seems to exert a longer and more effective protection.

3.2. *Deaerated sodium chloride solution*

In the NaCl deaerated solution only two cathodic reactions are possible: the diffusion controlled proton reduction:

$$2H_3O^+ + 2e^- = H_2 + 2H_2O \qquad (1)$$

and the water reduction, under activation control:

$$2H_2O + 2e^- = 2OH^- + H_2 \qquad (2)$$

Baugh [29] showed that, in simple salt solutions like NaCl, the cathodic current close to the corrosion potential is due predominantly to diffusion controlled proton reduction. Water reduction also occurs in the whole range of cathodic polarization.

The impedance diagrams relevant to different zinc electrodeposits always show the presence of a Warburg impedance related to Reaction 1; nevertheless the Warburg impedance coefficient σ ($\Omega s^{1/2}$) [21] changes considerably from one sample to the other, probably as a function of the zinc surface conditions (purity grade of the deposit, microcrystalline texture, presence of oxidized compounds). It can be assumed that water reduction occurs more easily at the corrosion potential, as a function of the chemical and microstructural characteristics of the zinc surface, so that the impedance diagram can change when either Reaction 1 or 2 predominates. In the case of a charge transfer controlled mechanism (Fig. 4a and Table 2), it is possible to extrapolate the R_{ct} data on the real impedance axis, obtaining a value of about $2700\,\Omega cm^2$. This value is higher in comparison to that obtained in aerated conditions as a consequence of the decrease in the total cathodic current. For different samples, the real component of the impedance increases as diffusion control becomes the rate determining step. The electrochemical behaviour of the zinc electrodeposit is constant during the 24 h of immersion.

The shape of the impedance diagrams relevant to the other studied materials also depends on the competition between the two possible reactions expressed

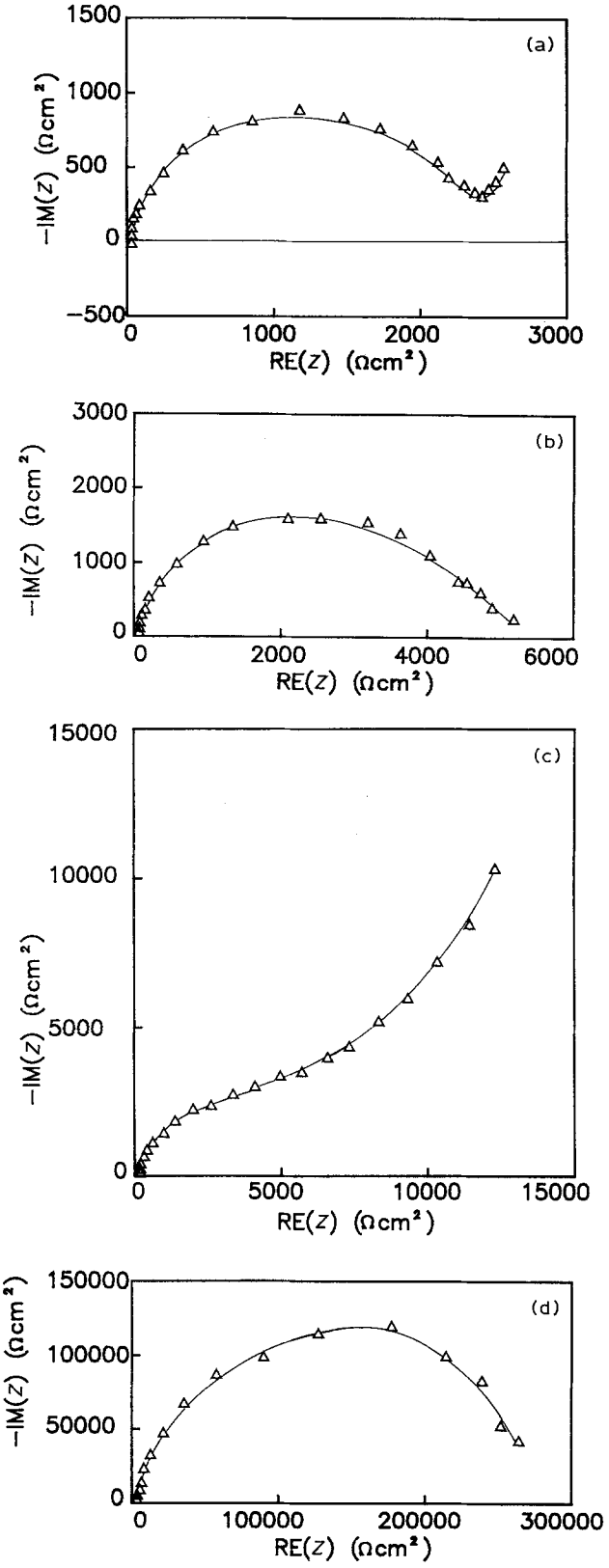

Fig. 4. Nyquist impedance plots obtained in deaerated 3.5% NaCl solution (a) Zinc, (b) zinc–nickel, (c) chromated zinc and (d) chromated zinc–nickel.

in 1 and 2 (above). The impedance plots of the zinc–nickel electrodeposits (Fig. 4b) never showed a Warburg impedance. To justify such an experimental trend, it can be assumed that the water reduction, activation controlled, occurs more easily on the nickel sites [30], becoming the main cathodic reaction. Under stationary conditions the R_{ct} values are of about $5000\,\Omega\,cm^2$ and remain almost unchanged during the immersion time. As observed before, R_{ct} is higher compared to the aerated conditions due to the absence of oxygen reduction.

The impedance diagram relevant to the passivated zinc electrocoatings (Fig. 4c) shows the presence of a clear Warburg impedance which can be related predominantly to diffusion control, probably because water reduction occurs with difficulty on the chromate film. In the deaerated solution, the corrosion resistance of the chromate coating increases and no degradation is observed during the immersion time.

The impedance plots relevant to the passivated zinc–nickel electrodeposits (Fig. 4d) do not show any change compared with those obtained in the aerated condition. Therefore the very good corrosion resistance of this material in the NaCl solutions, and the fact that the cathodic reactions are not a rate determining step in this case is confirmed. The R_{ct} values remain very high during the immersion time.

3.3. *Aerated ammonium sulphate solution*

The impedance spectra obtained in the aerated 0.1 M $(NH_4)_2SO_4$ solution differ substantially from those measured in NaCl, due to different corrosion mechanisms (Fig. 5 and Table 3). In this environment, the double layer at cathodic potentials will mainly consist of NH_4^+ ions whose electroactivity may be either direct [13]:

$$\begin{aligned} NH_4^+ + e^- &= NH_3 + H \\ H + H_3O^+ + e^- &= H_2 + H_2O \end{aligned} \qquad (3)$$

or indirect

$$\begin{aligned} NH_4^+ + H_2O &= NH_3O^+ + NH_3 \\ 2H_3O^+ + 2e^- &= H_2 + H_2O \end{aligned} \qquad (4)$$

Moreover, the NH_4^+ ions present in the double layer have the ability to inhibit oxide film formation [31] and give support to the theory that in ammonium salt solutions the local pH at the zinc surface is sufficiently low to inhibit film formation.

The impedance diagrams show an inductive loop which is clearly detectable on high purity zinc electrodeposits and decreases or disappears on industrial or alloyed zinc coatings [32]. In the presence of an inductive loop the R_p value is different from the R_{ct} value [33]. For the zinc electrocoatings, the R_p is of about $1800\,\Omega\,cm^2$ during the first immersion hours and it decreases after 24 h reaching the value of about $600\,\Omega\,cm^2$ (Fig. 5a). The decrease in R_p, contrary to the trend observed in NaCl solution, confirms that the ammonium solution is able to dissolve the oxide compounds present on the zinc surface and to inhibit the formation of films of corrosion products so increasing zinc corrosion. Moreover, the C_{dl} values are different from those observed in NaCl, confirming the different structure of the double layer.

No inductive loop is present in the impedance plots related to zinc–nickel samples (Fig. 5b); the R_{ct} value

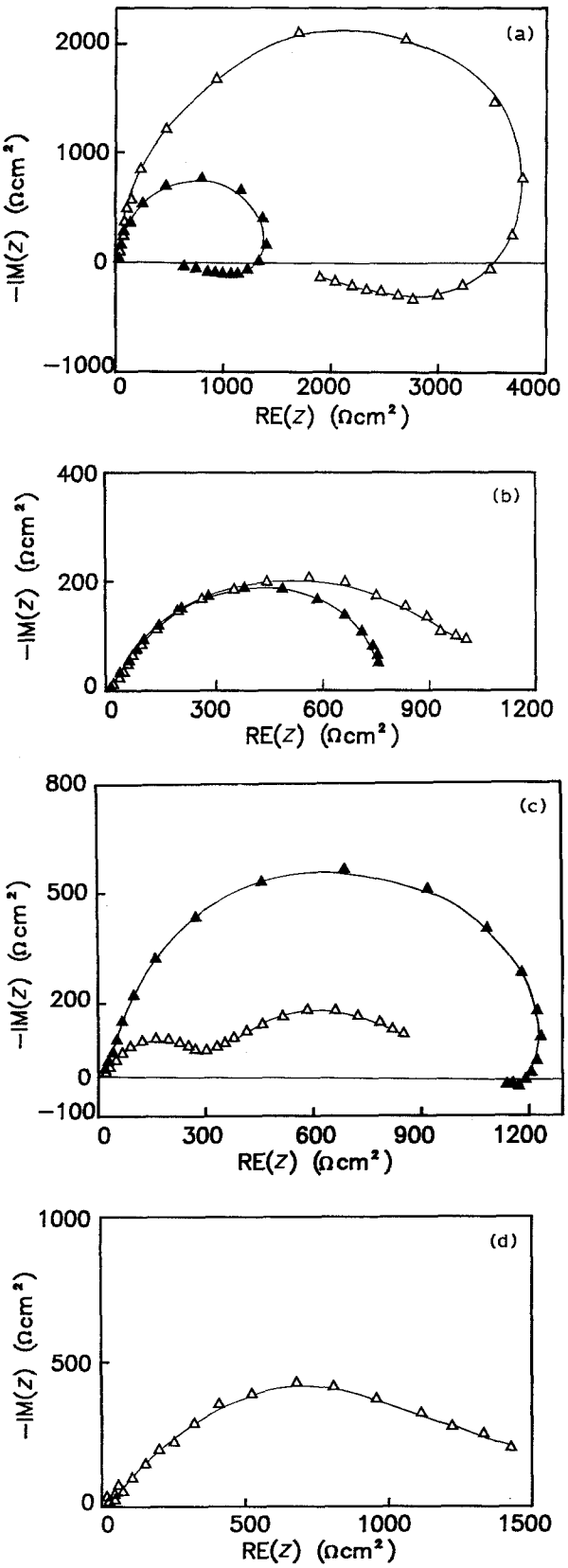

Fig. 5. Nyquist impedance plots obtained in aerated 0.1 M $(NH_4)_2SO_4$ solution after 3 (△) and 24 (▲) hours of immersion. (a) Zinc, (b) zinc–nickel, (c) chromated zinc and (d) chromated zinc–nickel.

ranges from 1100 to 750 Ωcm^2 during the 24 h of immersion and the alloy corrosion rate appears enhanced in the ammonium salt solution compared to the sodium chloride one. In fact, on the zinc–nickel electrodeposits, the corrosion mechanism is mainly supported by the hydrogen evolution reaction which occurs very easily, as confirmed by the visual observation of gas evolution on the surface of these electrocoatings at open circuit. As a consequence of the changed corrosion mechanism, the zinc–nickel alloy in ammonium solution does not show any corrosion resistance improvements compared to the zinc electrocoatings, contrary to the results obtained in the sodium chloride solution.

Table 3. Polarization resistance, R_p (Ωcm^2), resistance, $R(\Omega cm^{-2})$ and capacity, $C(\mu F cm^{-2})$ values derived from the impedance spectra obtained in aerated and deaerated 0.1 M $(NH_4)_2SO_4$ solutions.

Material	*Time (h)*	*Aerated*			*Deaerated*	
		R_p	R	C	R	C
Zn	3	1800	3800	0.66	10000	10
	24	600	1400	1.8		
Zn–Ni	3		1100	57.8	750	10
			750	848		
Chromated Zn	3		300*	8.4*		
					15000	10.6
	3		600	2652		
	24	1100	1300	4.87		
Chromated Zn–Ni	3		1400	56	1100	58
	24					

* Impedance diagram showing two capacitative loops.

The behaviour of the passivated zinc (Fig. 5c) or zinc–nickel (Fig. 5d) electrodeposits is also clearly influenced by the local surface acidity. The impedance spectra show that the chromate coating protection fails rapidly on both the samples, the electrochemical behaviour becoming similar to that of the untreated electrodeposit. Also, during the immersion time, a small inductive loop appears for the passivated zinc electrocoating. As a consequence of the fast dissolution of the chromate coating, no corrosion resistance improvements can be determined for the passivated electrocoatings compared to the untreated ones, in the ammonium sulphate solution.

3.4. *Deaerated ammonium sulphate solution*

In the deaerated ammonium sulphate solution, the cathodic reactions are mainly supported by the hydrogen evolution reaction, involving the NH_4^+ ion reduction. The zinc electrodeposit (Fig. 6a and Table 3) shows a charge transfer controlled corrosion mechanism; in fact the impedance diagram shows, after some hours of immersion, a very wide capacitative loop with R_{ct} values in the order of $10^4 \Omega cm^2$. This trend, completely different from that observed in the aerated condition, indicates that the oxygen cathodic reduction is the most important reaction in the aerated solution and that the hydrogen reduction involving NH_4^+ ions can occur in the deaerated condition, but with a high overvoltage on the zinc surface.

The same trend is observed on the passivated zinc electrodeposits (Fig. 6c), which also show, in the

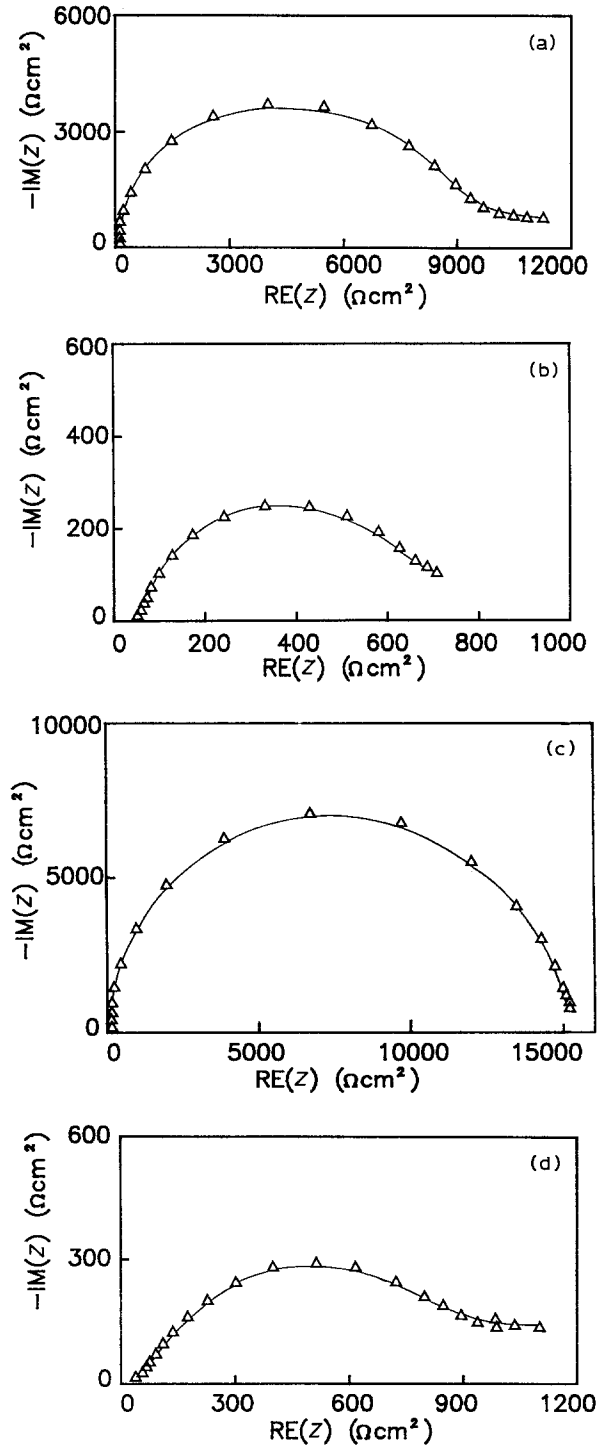

Fig. 6. Nyquist impedance plots obtained in deaerated 0.1 M $(NH_4)_2SO_4$ solution. (a) Zinc, (b) zinc–nickel, (c) chromated zinc, and (d) chromated zinc–nickel.

deaerated solution, rapid dissolution of the chromate coating. This trend confirms that the chromate film degradation depends on the local surface pH decrease, induced by the ammonium ion activity. By contrast, in the deaerated solution, the zinc–nickel alloy does not show any remarkable variation of the impedance spectra in comparison with the aerated condition (Fig. 6b). Thus, it can be supposed that the oxygen presence has a small influence on the total cathodic current, which is mainly supported by Reactions 3 and 4, the hydrogen reduction occurring easily on nickel containing surfaces.

The poor resistance of the chromate coatings in the ammonium sulphate solution is confirmed by the impedance plots relevant to the passivated zinc–nickel alloys (Fig. 6d). In fact these materials also show fast dissolution of the chromate films, and after very few hours of immersion the electrochemical behaviour becomes the same as that of the untreated zinc–nickel electrodeposits.

4. Conclusion

The use of the EIS allows the corrosion behaviour of electrogalvanized steel samples to be characterized. In sodium chloride solution the zinc–nickel electrodeposit shows a better corrosion resistance in comparison with the pure zinc coating during the immersion time. A surface nickel enrichment which, together with the zinc corrosion products, acting as a barrier layer reducing the total corrosion rate was observed. In the deaerated solution both the zinc and zinc–nickel electrodeposits show high polarization of the cathodic reactions, with an actual reduction in the corrosion rate. Moreover, on the zinc surfaces the corrosion mechanism is under diffusion or activation control depending on the chemical and microstructural condition of the surface.

The passivation treatment improves the corrosion resistance of the electrodeposits; nevertheless, on zinc substrates, the protection offered by the chromate film is not always effective during the immersion time. On the contrary, the chromate coatings on zinc–nickel substrates induce a remarkable and durable improvement of the corrosion behaviour, reducing the zinc dissolution almost completely.

In the ammonium sulphate solution, the corrosion mechanism is influenced by the hydrogen reduction which is favoured by the presence of NH_4^+ ions. This cathodic reaction is particularly effective on the zinc–nickel surface, enhancing the corrosion rate of this alloy. In the deaerated solution also, the corrosion mechanism of the zinc–nickel alloy is supported by the NH_4^+ ions reactions, and no lowering of the corrosion rate was observed. However, the zinc electrodeposit showed a high overvoltage with respect to this cathodic reaction, so that the corrosion behaviour is improved in the deaerated ammonium sulphate solution.

The ammonium sulphate solution, seems to be particularly aggressive for the chromate coatings due to the production of surface acidity. Therefore, both in aerated and deaerated solutions, the passivated zinc or zinc–nickel deposits show a fast dissolution of the chromate films, demonstrating the same corrosion behaviour as the substrate materials after very few immersion hours.

Acknowledgements

The research was supported by MURST and by the National Research Council of Italy.

References

[1] A. Catanzaro, G. Arrigoni, M. Palladino and M. Sarracino, 'SAE Technical Papers Series' No. 830583, Detroit, MI (1983), p. 107.

[2] M. Memmi, R. Bruno and M. Palladino, *Mater. Perform.* **2** (1983) 9.

[3] T. Adaniya, *Sheet Metal Ind. Int.* **12** (1987) 73.

[4] T. Adaniya, M. Omura, K. Matsudo and H. Naemura, *Plat. Surf. Finish.* **68** (1981) 96.

[5] R. Fratesi and G. Roventi, *Mat. Chem & Phys.* **23** (1989) 529.

[6] K. Higashi, H. Fukoshima, T. Urokawa, T. Adaniya and K. Matsudo, *J. Electrochem. Soc.* **128** (1981) 2081.

[7] T. Watanabe, M. Omura, T. Honma and T. Adaniya, 'SAE Tech. Pap. Series' No. 820424, Detroit, MI (1982).

[8] A. Shibuya, T. Kurimoto, K. Korekawa and K. Noji, *Tetsu to Hagane* **66** (1980) 771.

[9] V. Raman, M. Pushpavanam, S. Jayakirshnan and B. A. Shenoi, *Met. Finish.* **81** (1983) 85.

[10] D. E. Hall, *Plat. Surf. Finish.* **71** (1983) 59.

[11] G. F. Hsu, *ibid.* **71** (1984) 52.

[12] L. Felloni, R. Fratesi, E. Quadrini and G. Roventi, *J. Appl. Electrochem.* **17** (1987) 574.

[13] L. M. Baugh, *Electrochim. Acta* **24** (1979) 669.

[14] C. Cachet and R. Wiart, *J. Electroanal. Chem.* **129** (1981) 103.

[15] C. Deslouis, M. Duprat and C. Tournillon, *Corr. Sci.* **29** (1989) 13.

[16] L. Felloni, R. Fratesi, G. Roventi and L. Fedrizzi, Proceedings of the 11th International Corrosion Congress, Florence, Italy, 2–6 April 1990 (edited by A.I.M., Milan). Vol 2, p. 365.

[17] W. J. Lorenz and F. Mansfield, *Corr. Sci.* **21** (1981) 647.

[18] L. Felloni, R. Fratesi and G. Roventi, Proceedings of XXII International Metals Congress, Bologna, Italy (ed. A.I.M., Milan), (1988) p. 687.

[19] R. Fratesi, G. Roventi and L. Fedrizzi, Proceedings of the XXIII A.I.M. National Congress, September 1990, Ancona, Italy (ed. A.I.M., Milan) p. 417.

[20] M. R. Lambert, R. G. Hart and H. E. Townsend, 'SAE Tech. Pap. Series' No. 831817, Detroit, MI (1983) p. 81.

[21] G. W. Walter, *Corr. Sci.* **26** (1986) 681.

[22] F. Mansfield, W. Kendig and S. Tsai, *Corrosion* **38** (1982) 570.

[23] T. Hurlen and K. P. Fischer, *J. Electroanal. Chem.* **61** (1975) 165.

[24] J. T. Kim and J. Jorné, *J. Electrochem. Soc.* **127** (1980) 8.

[25] P. L. Bonora, Proceedings of the XIX Fatipec Congress, September 1988, Aachen, Germany (ed. Ungeheuer-Ulmer), (1988) vol. IV, p. 1.

[26] C. Deslouis, M. Duprat and C. Tulet-Tournillon, *J. Electroanal. Chem.* **181** (1984) 119.

[27] G. Trabanelli, F. Zucchi, G. Brunoro and G. Gilli, *Surf. Technol.* **3** (1975) 129.

[28] R. L. Zeller III and R. F. Savinell, *Corr. Sci.* **26** (1986) 389.

[29] L. M. Baugh, *Electrochim. Acta* **24** (1979) 657.

[30] A. J. Bard, 'Encyclopedia of Electrochemistry of the Elements', vol. IX part A, Marcel Dekker, New York (1975) p. 523.

[31] L. M. Baugh, J. A. Lee, *J. Electroanal. Chem.* **48** (1973) 55.

[32] L. Fedrizzi, G. Biscaglia and P. L. Bonora (submitted to *Br. Corros. J.*).

[33] I. Epelboin, C. Gabrielli, M. Keddam and H. Takenouti, *Electrochim,. Acta* **20** (1975) 913.